Plant Cell Rep
DOI 10.1007/s00299-016-2039-2

ORIGINAL ARTICLE

Virus-induced gene silencing (VIGS)-mediated functional characterization of two genes involved in lignocellulosic secondary cell wall formation

Shashank K. Pandey[1] · Akula Nookaraju[1,2,4] · Takeshi Fujino[1] · Sivakumar Pattathil[3] · Chandrashekhar P. Joshi[1,2]

Received: 11 April 2016 / Accepted: 9 August 2016

Abstract

Key message **Functional characterization of two tobacco genes, one involved in xylan synthesis and the other, a positive regulator of secondary cell wall formation, is reported.**

Abstract Lignocellulosic secondary cell walls (SCW) provide essential plant materials for the production of second-generation bioethanol. Therefore, thorough understanding of the process of SCW formation in plants is beneficial for efficient bioethanol production. Recently, we provided the first proof-of-concept for using virus-induced gene silencing (VIGS) approach for rapid functional characterization of nine genes involved in cellulose, hemicellulose and lignin synthesis during SCW formation. Here, we report VIGS-mediated functional characterization of two tobacco genes involved in SCW formation. Stems of VIGS plants silenced for both selected genes showed increased amount of xylem formation but thinner cell walls than controls. These results were further confirmed by production of stable transgenic tobacco plants manipulated in expression of these genes. Stems of stable transgenic tobacco plants silenced for these two genes showed increased xylem proliferation with thinner walls, whereas transgenic tobacco plants overexpressing these two genes showed increased fiber cell wall thickness but no change in xylem proliferation. These two selected genes were later identified as possible members of *DUF579* family involved in xylan synthesis and *KNAT7* transcription factor family involved in positive regulation of SCW formation, respectively. Glycome analyses of cell walls showed increased polysaccharide extractability in 1 M KOH extracts of both VIGS-*NbDUF579* and VIGS-*NbKNAT7* lines suggestive of cell wall loosening. Also, VIGS-*NbDUF579* and VIGS-*NbKNAT7* lines showed increased saccharification rates (74.5 and 40 % higher than controls, respectively). All these properties are highly desirable for producing higher quantities of bioethanol from lignocellulosic materials of bioenergy plants.

Keywords Secondary cell wall (SCW) · Saccharification · Bioethanol production · Transcriptional regulation · Virus-induced gene silencing (VIGS) · Xylan synthesis

Communicated by E. Guiderdoni.

S. K. Pandey and A. Nookaraju contributed equally to this work.

Electronic supplementary material The online version of this article (doi:10.1007/s00299-016-2039-2) contains supplementary material, which is available to authorized users.

✉ Chandrashekhar P. Joshi
cpjoshi@mtu.edu

[1] Department of Bioenergy Science and Technology, Chonnam National University, Gwangju 500-757, South Korea

[2] Department of Biological Sciences and School of Forest Resources and Environmental Science, Michigan Technological University, Houghton, MI 49931, USA

[3] Complex Carbohydrate Research Center, University of Georgia, 31, Riverbend Road, Athens, GA 30602, USA

[4] Present Address: Kaveri Seed Company Ltd., Minerva Complex, Secunderabad 500003, India

Introduction

Plant cells are delimited by cell walls. The primary cell wall mainly consists of cellulose, hemicellulose, pectin and glycoproteins, whereas some specialized cells like xylem vessels, tracheids and fibers contain an additional wall, the secondary cell wall (SCW) that is largely composed of

Published online: 13 August 2016

cellulose, hemicellulose and lignin. The middle lamella, rich in pectins, joins and holds adjacent plant cells together. Cell walls play many important roles in plant's life: helping in cell adhesion and expansion, acting as a barrier to attack by pests and pathogens, and determining the physical properties of the plant (Braam 1999; Jones and Takemoto 2004; Scheible and Pauly 2004; Vorwerk et al. 2004). Apart from providing dietary fiber for human and animal consumption and raw materials for textile, paper and pulp industries, plant cell walls also play an important role in human lives by providing raw materials for the production of biofuels (Nookaraju et al. 2013). Yong et al. (2005) estimated that more than 1000 genes encoding cell wall-related proteins could be involved in cell wall formation, and that an equal number of unannotated genes might be functional in cell wall assembly and disassembly in plants. Virus-induced gene silencing (VIGS) is a simple, rapid and highly efficient approach for quick assessment of plant gene functions. It is a transient *RNAi*-mediated gene silencing method that facilitates fast and easy assessment of gene function that could be later confirmed by generating stable transgenics (Burch-Smith et al. 2004). VIGS system has been successfully used for addressing biological questions related to plant defense, development, and metabolism in many plant species (Lu et al. 2003; Burch-Smith et al. 2004; Robertson 2004). Previously, we successfully used this system for the first time to silence *Nicotiana benthamiana* (*N. benthamiana*) homologues of nine Arabidopsis cell wall genes (three genes each involved in cellulose, xylan and lignin pathways) and demonstrated that VIGS plants exhibited the expected morphological phenotypes, altered anatomy and cell wall chemistry (Zhu et al. 2010). In the present study, we employed the same tobacco rattle virus (TRV)-based VIGS system for further understanding the function of two genes involved in SCW formation. Furthermore, we also characterized the functions of these two genes by generating stable *RNAi* and overexpression transgenic lines.

By surveying the literature on xylem development in various plant species, we first identified 38 gene targets for VIGS screening. This list included genes encoding various unknown function proteins and some transcription factors. Among these, two genes when silenced using VIGS technique showed interesting phenotype of massive xylem proliferation and were selected for further functional studies. These two genes were later identified as members of *DUF579* family and *KNAT7* transcription factor family, respectively, based on their homology with Arabidopsis genes. While this work was in progress, the functions of these two genes were reported in Arabidopsis (Brown et al. 2011; Jensen et al. 2011; Li et al. 2012). Based on these reports, the *DUF579* gene appears to be involved in xylan synthesis and *KNAT7* gene is likely to be a negative regulator of SCW deposition. However, the phenomenon of xylem proliferation that we observed in tobacco was not observed by silencing either of these genes in Arabidopsis. In the present study, we observed that gene *NbDUF579* is involved in xylan synthesis but *NbKNAT7* gene is a positive regulator of SCW formation in tobacco. Furthermore, downregulation of these two genes in transgenic tobacco, through VIGS and *RNAi* system, resulted in decreased cell wall thickness and increased xylem proliferation with overall alteration in cell wall extractability as observed by glycome analysis and increase in sugar release (saccharification) efficiency. Whereas overexpression lines of *NbDUF579* and *NbKNAT7* genes showed increased cell wall thickness compared to control plants, but no alteration in xylem proliferation was observed. All these observations have direct implications in efficient bioethanol production (Nookaraju et al. 2013).

Materials and methods

VIGS vector construction

Tobacco (*N. benthamiana*) orthologs of *Arabidopsis DUF579* and *KNAT7* genes were PCR-amplified using gene-specific primers (Table S1). Resulting gene fragments were cloned into VIGS vector *pTRV2-LIC*, and transferred to *Agrobacterium* strain GV2260 using freeze–thaw method (Dong et al. 2007).

Plant transformation and growth conditions

For VIGS experiment, *N. benthamiana* plants were grown under continuous light at 25 ± 1 °C for 3 weeks. *Agrobacterium* strain GV2260 containing *pTRV1*, *pTRV2-LIC* (control), and modified *pTRV2-LIC* vectors for silencing gene *NbDUF579* and *NbKNAT7* was grown in Luria broth (LB) medium containing kanamycin (50 mg L^{-1}) and rifampicin (25 mg L^{-1}) at 28 °C for overnight. Next day, cells were pelleted and re-suspended in the infiltration medium (10 mM MES, 10 mM $MgCl_2$, 200 µM acetosyringone) to a final OD_{600} of 1.0. Prior to infiltration, *Agrobacterium* cell suspensions were incubated at room temperature for 3 h (Zhu and Dinesh-Kumar 2008). Then, tobacco leaves were infiltrated with 1:1 cell suspension of *Agrobacterium* carrying *pTRV1* and modified *pTRV2-LIC* vector with a needleless syringe through leaf abaxial surface as described earlier (Zhu et al. 2010). Control plants were infiltrated with 1:1 mixture of *pTRV1* and *pTRV2-LIC* control vector. Infiltrated plants were grown at 25 ± 1 °C under continuous light. The experiment was repeated at least three times with four plants at each time.

Generation of stable transgenic lines

For *RNAi* study, *NbDUF579* and *NbKNAT7* gene fragments were PCR-amplified from *N. benthamiana* cDNA with gene-specific primers (Table S1) that contain XhoI + XbaI and KpnI + ClaI restriction sites on either sides, respectively, and cloned into the pTOP Blunt V2 vector (Enzynomics, Korea). After sequence confirmation, both the gene fragments were digested and sub-cloned into sense and antisense direction in *pHANNIBAL* vector as described earlier (Wang et al. 2004). Resulting *pHANNIBAL* constructs were digested with NotI, and *RNAi* cassettes were cloned into *pART27* binary vector used for plant transformation. Plasmid constructs of *pART-NbDUF579* (*pART27* vector with gene *NbDUF579*) and *pART-NbKNAT7* (*pART27* vector with gene *NbKNAT7*) were transformed into *Agrobacterium tumefaciens* strain GV2260 by freeze–thaw method.

For overexpression, full-length *N. benthamiana* cDNAs for *NbDUF579* and *NbKNAT7* genes were PCR-amplified using gene-specific primers (Table S1) that contain XbaI and SacI restriction sites on either sides and sub-cloned into pTOP Blunt V2 vector (Enzynomics, Korea). The plasmids were digested with XbaI and SacI to obtain full-length cDNAs of *NbDUF579* and *NbKNAT7* genes, and were cloned into *pBIN121* binary vector replacing β-*glucuronidase* (GUS) driven by CaMV 35S promoter. Plant transformation of tobacco (*N. benthamiana*) was carried out using leaf disks as explants by *Agrobacterium*-mediated gene transfer method (Pogrebnyak et al. 2005). Transgenic shoots were selected on kanamycin (50 μg mL^{-1}) and were rooted on half-strength MS medium containing kanamycin (50 μg mL^{-1}). The rooted shoots were then transferred to commercial potting mixture (3:2:1, peat:soil:perlite; Heung Nung Seeds, Korea), and the hardened plants were established in a growth room maintained at 25 ± 1 °C temperature and 50 % relative humidity.

RNA extraction and RT-PCR analysis

Total RNA was extracted from the stems (1–7 internodes counted from the base in plants with seven internodes) using RNeasy plant mini kit (Qiagen). First-strand cDNA was synthesized from 1 μg of total RNA using SuperScript reverse transcriptase kit (Invitrogen). qRT-PCR was performed using SYBR Green kit (Takara, Japan). The transcript abundance of all the genes was examined using gene-specific primers shown in Table S1.

Microscopic image analysis

For light microscopy, stems of VIGS plants were cut at the third internode from the base of plants with seven internodes and were fixed in 4 % PFA (paraformaldehyde) solution overnight. After fixation, internodes were dehydrated through ethanol and t-butanol series, and finally embedded in wax. Five-micrometer-thick sections were cut with a microtome, mounted on a slide and de-waxed. De-waxed sections were stained with Toluidine Blue O (TBO) and photographed using a light microscope. For measuring cell wall thickness, stem tissues were prepared in LR-white resin (London Resin Co., England) and sectioned at 0.5 μm using ultramicrotome and photographed.

Immunolocalization of xylan and xyloglucan were carried out using LM10 and LM15 monoclonal antibodies (Plant Probes) that recognize unsubstituted and relatively low substituted xylans (McCartney et al. 2005) and the XXXG motif of xyloglucan (Marcus et al. 2008), respectively, followed by incubation with fluorescein isothiocyanate (FITC)-conjugated secondary antibody (Sigma). The FITC-labeled sections were observed and photographed under a Zeiss Axiovert 200M inverted microscope equipped with an AxioCam fluorescence camera.

Glycosyl compositional analysis by GC–MS of TMS derivatives of methyl glycosides

Glycosyl compositional analysis was performed by combined gas chromatography/mass spectrometry (GC/MS) of the per-*O*-trimethylsilyl (TMS) derivatives of the monosaccharide methyl glycosides produced from the wood sample (stems consisting of seven internodes from the base) by acidic methanolysis as described earlier (Merkle and Poppe 1994; York et al. 1986). The sample (400–500 μg each) was placed in a separate tube with 20 μg of inositol as internal standard. Dry samples were hydrolyzed with 2 M TFA at 120 °C for 1 h. Hydrolysis products were dried by adding isopropanol. Methyl glycosides were then prepared from the dry sample by methanolysis with 1 M HCl methanol at 80 °C (16 h), followed by re-*N*-acetylation with pyridine and acetic anhydride in methanol (for detection of amino sugars). The samples were then per-*O*-trimethylsilylated by treatment with Tri-Sil (Pierce) at 80 °C (30 min). GC/MS analysis of the TMS methyl glycosides was performed on an Agilent 7890A GC interfaced to a 5975C MSD, using a Supelco EC-1 fused-silica capillary column (30 m × 0.25 mm ID). Data were collected and processed by Agilent ChemStation software.

Sequential extraction and glycome profiling

Sequential extractions of cell walls and glycome profiling of plants were carried out according to the procedure described earlier (Pattathil et al. 2012; Zhu et al. 2010; DeMartini et al. 2011). Tobacco stem samples consisting of seven internodes from base were used for the analysis. Plant glycan-directed monoclonal antibodies (McAbs) were obtained from laboratory stocks (CCRC, JIM and MAC series) at the Complex Carbohydrate Research Center (available through CarboSource Services; http://www.carbosource.net) and BioSupplies (Australia) (BG1, LAMP). A detailed list of all McAbs used in this study has been described earlier (Pattathil et al. 2015).

Lignin analysis

Tobacco stem samples consisting of seven internodes from base were used for the analysis. Tobacco stem tissue powder samples were weighed (5 mg) in a small sample cup; pyrolyzed using a Pyrolyzer at 500 °C, and the residues were analyzed using molecular beam mass spectrometer (Evans and Milne 1987). Each sample was analyzed in duplicates. The uncorrected lignin content was calculated using multivariate analysis (principal component analysis) and corrected with NIST 8492 (lignin = 26.2 %).

Cellulose estimation and sugar release

Tobacco stem samples consisting of seven internodes from base were used for the analysis. Tobacco stem tissue powders were treated with acetonitrile solution (acetic acid:nitric acid:water 8:2:1) at 100 °C for 30 min (Updegraff 1969). Then, the tissue powders were washed three times with sterile water and dried. The dried residue containing mostly cellulose was weighed and expressed in percentage. Sugar release was calculated using phenol–sulfuric acid method by monitoring the reactants' solution absorbance at 490 nm (Dubois et al. 1956). A glucose standard curve was prepared using 2–22 μg μL^{-1}, and glucose yields of tissue samples were calculated.

Phylogenetic analysis

Protein sequences of Arabidopsis for the two genes were obtained from The Arabidopsis Information Resource (TAIR; http://www.arabidopsis.org/), based on TAIR gene family annotations, and by BLASTP searches using KNAT7 and DUF579 as the queries. *N. benthamiana* protein sequences were retrieved by *N.benthamiana* Genome v1.0.1 Contigs (solgenomics.net/tools/blast/index.pl?db_id = 196). The draft genome sequence of *Nicotiana benthamiana* has been published (Bombarely et al. 2012). Protein sequences were aligned with Clustal Omega, and phylogenetic trees were generated using MEGA7 software. The evolutionary history was inferred using the neighbor-joining method. The percentage of replicate trees in which the associated taxa clustered together in the bootstrap test (500 replicates) is shown next to the branches. The tree is drawn to scale, with branch lengths in the same units as those of the evolutionary distances used to infer the phylogenetic tree. The evolutionary distances were computed using the Poisson correction method and are in the units of the number of amino acid substitutions per site.

Statistical analysis

Data from all experiments were analyzed statistically using one-way analysis of variance (ANOVA) followed by Scheffe's test for multiple comparisons (Scheffe 1959).

Results and discussion

Gene selection and study of expression of selected genes in tobacco

Among the 38 genes selected initially for functional screening using VIGS, two genes *NbDUF579* and *NbKNAT7* showed interesting phenotype of thinner fiber walls and increased xylem formation. Both the genes showed differential expression in various tissues of tobacco plants (Fig. S1). *NbDUF579* gene showed higher expression in older stems (OS) followed by younger stems (YS). The young leaf (YL), old leaf (OL) and root samples showed moderate expression, while flower (F) and petiole (P) samples showed very low expression (Fig. S1A). The *NbKNAT7* gene showed higher expression in old leaf (OL) followed by old stem (OS), young leaf (YL) and root (R) (Fig. S1B). Amino acid-based alignment of Arabidopsis and tobacco *DUF579* genes indicates that the two close members in tobacco, *DUF579* and *DUF579*-L are closely related to two Arabidopsis *DUF579* gene family members, *irx15* and *irx15-L* (Fig. S2A). Similarly, tobacco *NbKNAT7* gene is placed very close to its Arabidopsis counterpart (Fig. S2B).

Silencing of genes *NbDUF579* and *NbKNAT7* showed increased xylem formation and reduced wall thickness

To understand the functions of these genes, VIGS experiments were independently repeated followed by reconfirmation of those results by stable transformation of tobacco

plants with *RNAi* and overexpression constructs. The VIGS plants silenced for expression of genes, *NbDUF579* and *NbKNAT7* did not show any morphological variations and were highly similar to control plants in terms of plant height, internode number and stem girth (Fig. 1a, b). This is a highly desirable trait since transgenic plants altered in cell wall properties sometimes show negative effects on overall plant growth (e.g., Joshi et al. 2011). However, as expected, qRT-PCR expression results showed a significant downregulation of these genes in VIGS plants as compared to control (Fig. 1c). To examine whether similar to initial screening, these VIGS plants also have any changes in their xylem phenotype over control plants, the stems were hand-sectioned at third internode from base and examined under light microscope. We confirmed increased xylem formation (increased number of cell layers and higher proportion of xylem area) in stems of VIGS plants as compared to control plants, similar to what was observed in our preliminary studies, and the increase in xylem area was statistically significant (Fig. 2a). There were about 55 and 49 %

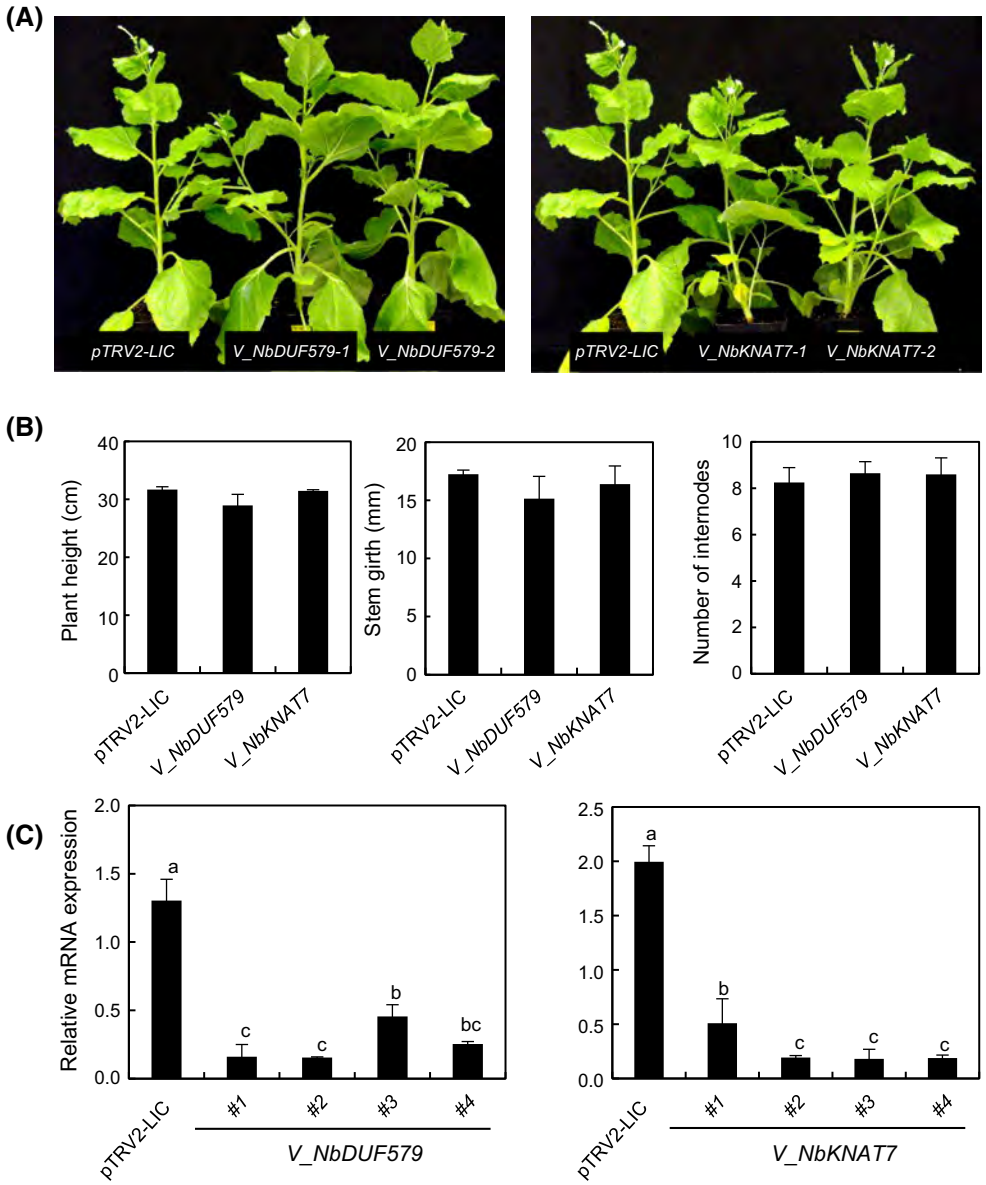

Fig. 1 Morphological analysis of tobacco plants silenced for *NbDUF579* and *NbKNAT7* genes through VIGS system. **a** Phenotype of VIGS-silenced plants, **b** analysis of plant height, stem girth and number of internodes of *V_NbDUF579* (*VIGS_NbDUF579*) and *V_NbKNAT7* (*VIGS_NbKNAT7*) and vector control (*pTRV2-LIC*) plants. **c** Relative mRNA expression levels of genes *NbDUF579* (**a**) and *NbKNAT7* (**b**) in stems of VIGS plants at 30 days after infiltration (DAI) indicating the reduction in transcript level. *Error bars* represent standard error (SE) of three independent experiments. Gene expression levels were compared with actin control. Bars denoted by the same letter are not significantly different ($p = 0.01$, ANOVA, post hoc Scheffe's test)

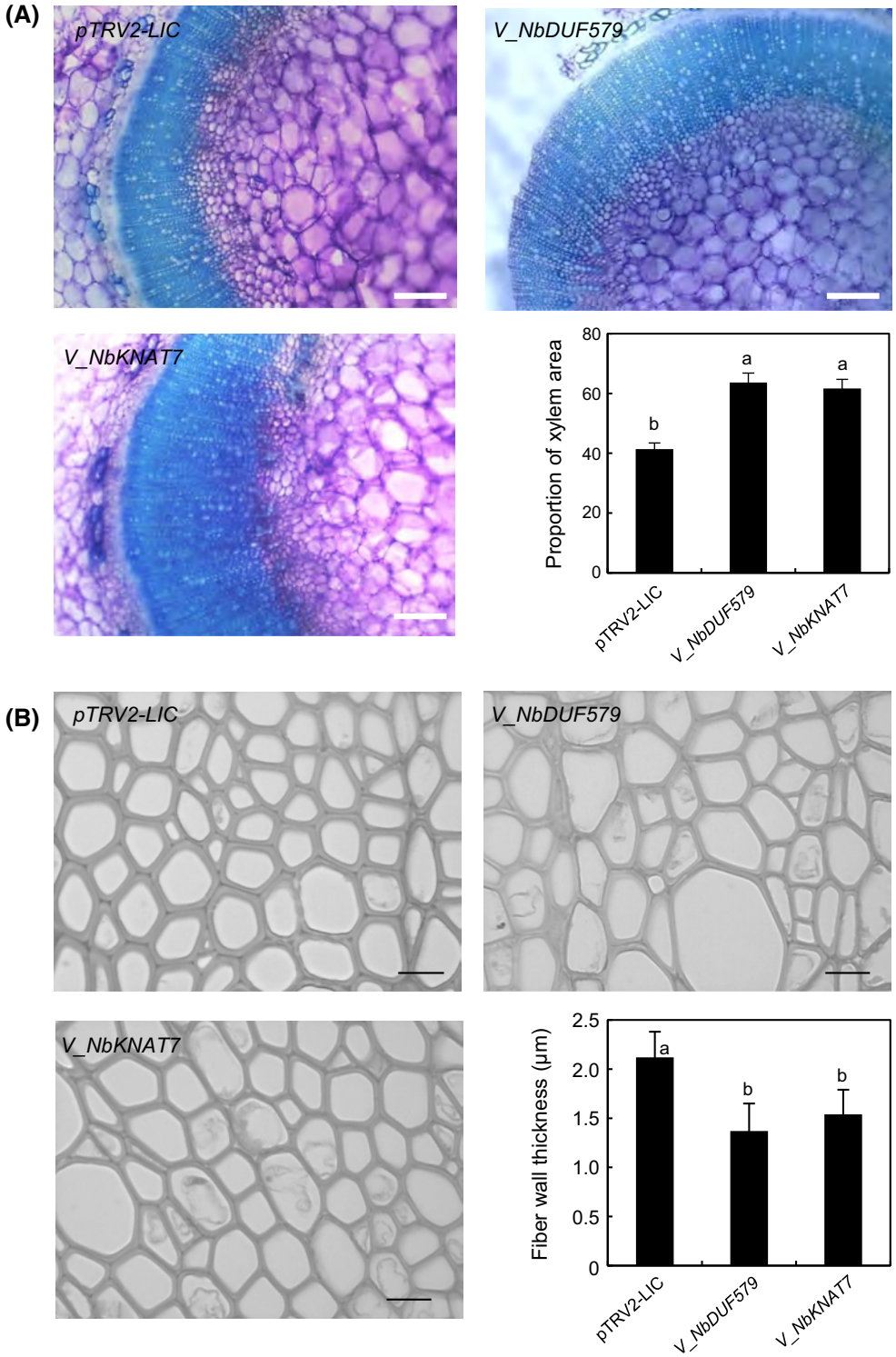

Fig. 2 Anatomical analysis of VIGS-silenced vs. vector control plants. **a** TBO-stained transverse sections (TS) of stems at third internode from base and proportion of xylem area in *V_NbDUF579* (*VIGS_NbDUF579*) and *V_NbKNAT7 (VIGS_NbKNAT7)* plants as compared to control. *Scale bars* 200 µm. Bars are mean ± SE of 12 samples. *Bars* denoted by the *same letter* are not significantly different ($p = 0.01$, ANOVA, post hoc Scheffe's test). **b** Fiber wall thickness in stems of 6-week-old control (*pTRV2-LIC*) and VIGS-silenced *NbDUF579* and *NbKNAT7* plants. *Scale bars* 5 µm. *Bars* are mean ± SE of 60 observations. *Bars* denoted by the *same letter* are not significantly different ($p = 0.01$, ANOVA, post hoc Scheffe's test)

increases in xylem area in stems of VIGS plants silenced for genes *NbDUF579* and *NbKNAT7*, respectively, over control stems. At the same time, xylem fiber wall thickness was reduced by 35 and 42 % in VIGS lines silenced for the genes *NbDUF579* and *NbKNAT7*, respectively, as compared to control plants (Fig. 2b). Increased xylem proliferation in gene-silenced lines could be partially attributed as a compensatory mechanism to reduced fiber cell wall thickness. Similar reduction in fiber cell wall thickness and increased xylem formation were also observed in stable *RNAi* lines of tobacco for genes, *NbDUF579* and *NbKNAT7* (Fig. 3a–c). Whereas opposite phenomenon was observed in overexpression (OX) lines of tobacco, where about 40 and 50 % increases in cell wall thickness were observed in tobacco lines overexpressing genes *NbDUF579* and *NbKNAT7*, respectively, over vector control lines (Fig. 3d, e). However, no change in xylem area was noticed in OX lines as compared to vector control plants.

The expression of target genes, *NbDUF579* and *NbKNAT7*, in their respective stable *RNAi* and overexpression lines is given as supplementary Fig. S3. While our studies were in progress, *NbDUF579* gene was reported to be involved in xylan biosynthesis in Arabidopsis stem (Brown et al. 2011; Jensen et al. 2011). Double mutants for two close members of AtDUF579 (*irx15 irx15-L*) showed irregular xylem (*irx*) phenotype in Arabidopsis stems. However, in our study, we did not observe any *irx* phenotype although we observed reduced cell wall thickness when gene *NbDUF579* was downregulated. This might be due to species-specific differences or partial silencing of the genes or due to the compensatory expression of other members of DUF579 family in tobacco. Similarly, in poplar, downregulation of poplar distant homolog *PtrDUF579-1* resulted in reduced cambial activity leading to reduced xylem area and reduced plant growth (Song et al. 2014). The phenomenon of xylem proliferation as observed in tobacco was also not reported in Arabidopsis and poplar. We found two members of *NbDUF579* gene family in recently completed *N. benthamiana* genome data (ftp://ftp.solgenomics.net/benthamiana) (Bombarely et al. 2012). The *RNAi* fragment used for VIGS study is expected to silence both these members based on their homology with the *RNAi* probe (Fig. S4A).

Identified *NbKNAT7* gene is a member of *AtKNAT7* (Class-II KNOX) transcription factor (TF) family and was recently reported to be a negative regulator of secondary cell wall biosynthesis in Arabidopsis based on *knat7* loss-of-function mutant data (designated as *irx11*) (Li et al. 2012). These mutants also displayed secondary cell wall thickening in interfascicular fiber cells and irregular xylem (*irx)* phenotype (Li et al. 2012). However, overexpression of *KNAT7* showed thinner interfascicular fiber cell walls. On the basis of different observations in Arabidopsis and poplar, it was demonstrated that *KNAT7* is a negative regulator of secondary wall biosynthesis in interfascicular fiber cells and functions in a negative feedback loop that represses metabolically inappropriate commitment to secondary wall formation to maintain the metabolic homeostasis as suggested by Li et al. (2012). In a recent study, Liu et al. (2014) reported that BLH6, a BELL1-LIKE HOMEODOMAIN protein, specifically interacts with KNAT7, and that this interaction influenced secondary cell wall development. BLH6 is a transcriptional repressor, and BLH6–KNAT7 physical interaction enhanced KNAT7 and BLH6 repression activities. Overexpression of BLH6 and KNAT7 resulted in thinner interfascicular fiber secondary cell walls. However, contrasting results were reported by Zhong et al. (2008) in Arabidopsis plants expressing engineered dominant repression variant of At-KNAT7. Dominant repression of *knat7* caused a severe reduction in secondary wall thickening in both interfascicular fibers and xylary fibers in inflorescence stems, and the severity of reduction correlated with the amount of the repression. Furthermore, the cell wall composition analysis of these repressor lines showed significantly reduced amount of glucose and xylose, the main sugars in cellulose and xylan, respectively. In our study, we observed thinner walls in VIGS-silenced lines for gene *NbKNAT7*, which indicates positive regulation of SCW genes by KNAT7 in secondary cell wall formation. This was accompanied by reduced expression of many downstream secondary cell wall genes in *KNAT7*-silenced tobacco lines (Fig. 4a, c, e). This is the result of silencing of a single *NbKNAT7* gene, while no silencing of *NbKNAT3,* its close member in the KNOX II family, was observed (Fig. S4B). In contrast, in overexpression lines, enhanced expression of secondary cell wall genes was observed (Fig. 4b, d, f). Taken together, our findings indicated that KNAT7 is a positive regulator of secondary wall biosynthesis in stems of tobacco.

Altered glycome profile of VIGS lines as compared to control indicate differences in cell wall composition

To ascertain the existence of variations in the cell wall composition, glycome profiling was performed on *VIGS-NbDUF579* and *-NbKNAT7* lines along with controls using the method reported earlier (Zhu et al. 2010). Overall, glycome profiles of *VIGS-NbKNAT7* lines were largely similar to those of control lines with subtle variations that reproduced among biological replicates (Fig. 5). Increased polysaccharide extractability was noticed in case of 1 M KOH extracts from *VIGS-NbKNAT7* lines (see top bar graphs Fig. 5, right panel). This observation suggests that cell walls are potentially loosened in the *VIGS-NbKNAT7*

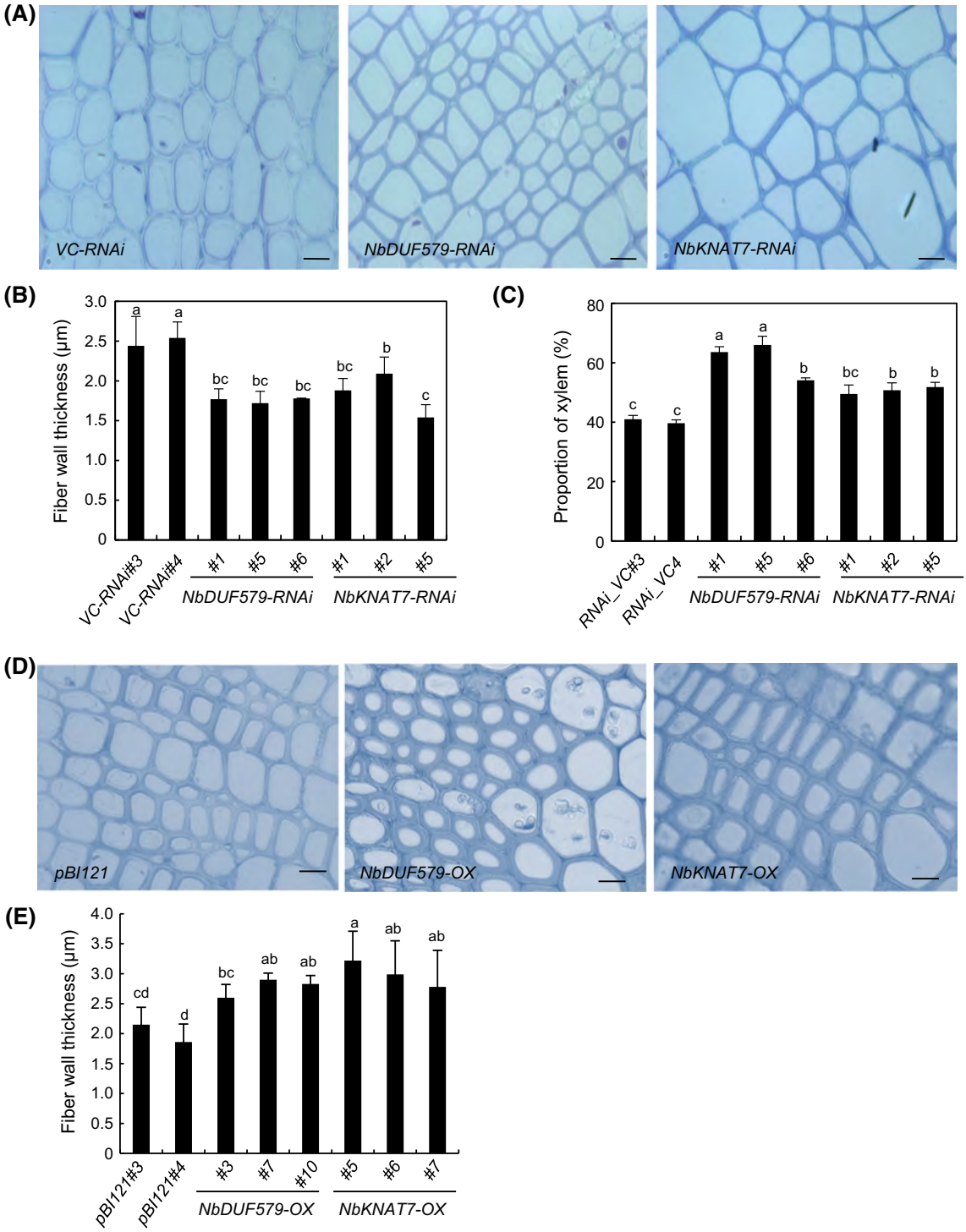

Fig. 3 Anatomical analysis of stable *RNAi* and OX transgenic plants. **a** Comparative anatomy of 6-week-old stems of vector control (VC) and stable *RNAi* lines silenced for *NbDUF579* and *NbKNAT7* genes. *Scale bars* 10 μm. **b**, **c** Fiber wall thickness in stems of control and *RNAi* lines. **d** Comparative anatomy of 6-week-old stems of vector control (pBI-VC) and overexpression (OX) lines for *DUF579* and *KNAT7* genes. Stem sections of vector control (*pBI*), *NbDUF579OX* and *NbKNAT7* lines of tobacco. *Scale bars* 5 μm. **e** Fiber wall thickness in stems of control and OX lines. *Bars* are mean ± SE of 60 observations. *Bars* denoted by the *same letter* are not significantly different ($p = 0.01$, ANOVA, post hoc Scheffe's test). Sections were taken at third internode from base (dia. 5.2 mm) and sections were stained with *toluidine blue*

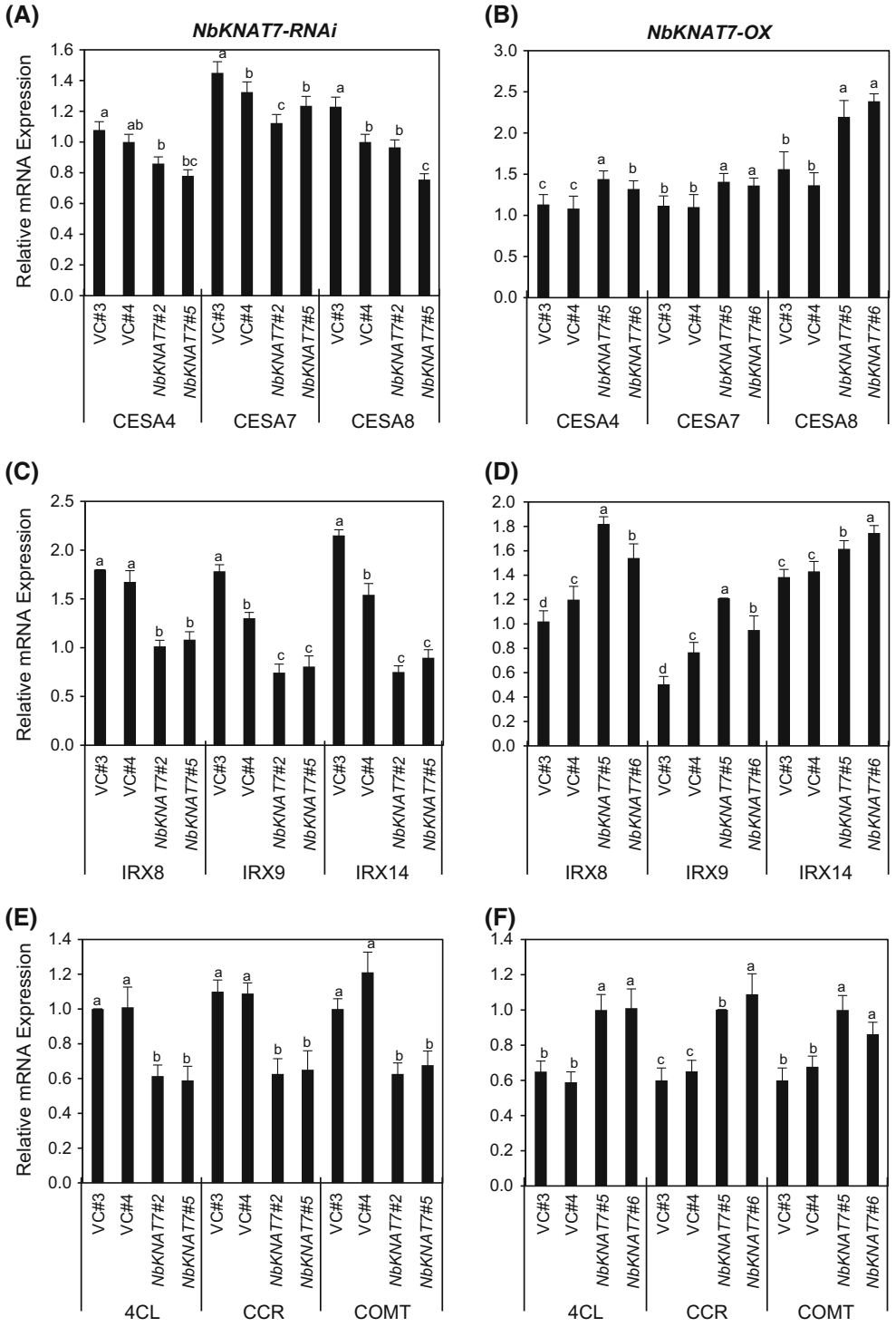

Fig. 4 Relative mRNA expression levels of secondary cell wall cellulose (**a**, **b**), hemicellulose (**c**, **d**) and lignin (**e**, **f**) genes in stems of tobacco *RNAi* (*left side*) and overexpression (*right side*) lines for gene *NbKNAT7* compared to vector control (VC) plants. *Error bars* represent SE of three independent experiments. Transgene expression levels were compared with actin control

lines as a result of the gene *KNAT7* knockdown. A reduced binding intensity of xylan-5 through seven groups of antibodies (McAbs) was observed in the carbonate extracts of *VIGS-NbKNAT7* lines when compared to the controls. In *VIGS-NbKNAT7* lines, the binding patterns of homogalacturonan backbone-1 (HG backbone-1) group of McAbs significantly changed in chlorite and post-chlorite 4 M KOH extracts. Again, in these lines, the overall binding of

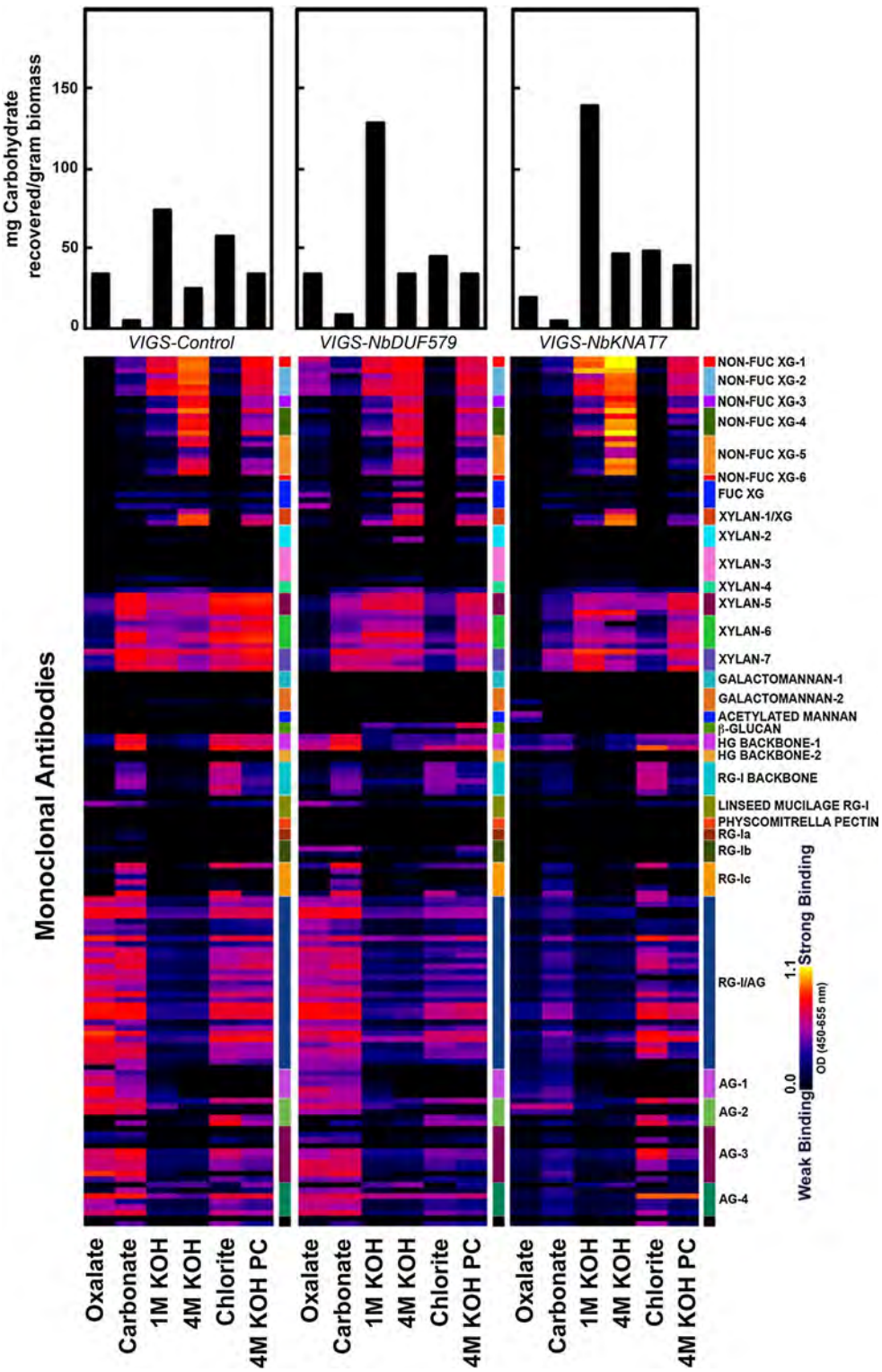

Fig. 5 Glycome profiling of cell walls from stems of control and *VIGS* lines. Sequential extracts of cell walls were made from stem tissues of *N. benthamiana* control and *VIGS* lines using ammonium oxalate, sodium carbonate and potassium hydroxide (1 M KOH and 4 M KOH), chlorite and post-chlorite 4MKOH as explained in methods section. The sequential extracts were subsequently screened with 155 mAbs directed against most major plant cell wall glycans. The ELISA binding response data are denoted as heat maps with *white-yellow-red-purple-blue-black scale* indicating the strength of the ELISA signal (*white*, *red* and *black colors* depict strong, medium, and no binding, respectively). The groupings of McAbs are based on their specificity to various cell wall glycans as shown in the *panel* at *right hand side* of the *figure*. The amounts of carbohydrate materials recovered out at each extraction are depicted as *bar graph* at the *top* of heat maps

pectic arabinogalactan-directed McAbs was notably reduced in chlorite and post-chlorite 4 M KOH extracts when compared to control lines. Together, these results show that virus-induced *NbKNAT7* gene silencing caused alterations in the extractability of glycan epitopes. Enhanced extractability of glycans in 1 M KOH fraction indicates reduced recalcitrance of these lines in terms of saccharification efficiency.

Similarly, glycome profiles of *VIGS-NbDUF579* lines were different than those of the control lines indicating

altered cell wall composition in these lines (Fig. 5). As observed in *VIGS-NbKNAT7* lines, the extractability of glycans by 1 M KOH was significantly higher in these lines than the controls. Notably reduced binding intensity of xylan-5 through seven groups of antibodies (McAbs) was observed in the carbonate extracts of *VIGS-NbDUF579* lines when compared to controls. In *VIGS-NbDUF579* lines also, the binding patterns of homogalacturonan backbone-1 (HG backbone-1) group of McAbs significantly changed in the case of chlorite and post-chlorite 4 M KOH extracts. Also, the overall presence of rhamnogalacturonan backbone-1 (RG backbone-1) epitopes was drastically reduced in carbonate extracts of *VIGS-NbDUF579* lines. The abundance of pectic arabinogalactan epitopes in oxalate and carbonate extracts of *VIGS-NbDUF579* lines significantly dropped in comparison to both control and *VIGS-NbDUF579* lines. Overall, these results indicate that virus-induced silencing of *NbDUF579* (DUF579 family member) caused alteration in the cell walls and, hence, changes in the extractability of wall glycan epitopes in tobacco. Significantly enhanced extractability of glycans in 1 M KOH indicates a reduced recalcitrance of these lines similar to *VIGS-NbKNAT7* lines.

Altered glycosyl composition and total carbohydrate contents

Individual monosaccharides were estimated from non-cellulosic cell wall fraction by TFA hydrolysis and methanolysis. The total yield of monosaccharides increased due to TFA hydrolysis conducted prior to methanolysis of the sample as compared to methanolysis alone. The composition of sugar monomers differed significantly between control and *VIGS-NbDUF579* lines (Table 1). Particularly, the amount of xylose significantly reduced in *VIGS-NbDUF579* lines indicating decreased polymerization of xylan backbone. At the same time, the levels of galacturonic acid (GalA), galactose, rhamnose and arabinose sugars increased which indicates increased xylan substitutions. Our results confirm the earlier findings in *Arabidopsis* xylan double mutant, *irx15 irx15-L* (Jensen et al. 2011; Brown et al. 2011). However, no *irx* phenotype was observed in tobacco stems. Apart from this, a substantial increase in glucose yield (>5 fold increase) was recorded in *VIGS-NbDUF579* lines as compared to vector control lines. This increase in glucose monomer yield indicates higher proportion of xyloglucan chains, which is a characteristic of primary walls. This shows substantial increase in the proportion of primary wall xylan in VIGS lines, which is evident from the increased amount of xylem area with higher number of fiber cells. Another possible reason for increased glucose yield could be the presence of more non-crystalline cellulose. However, *Arabidopsis* xylan double mutant, *irx15 irx15-L* did not show any reduction in crystalline cellulose content (Jensen et al. 2011).

In contrast to *VIGS-NbDUF579* lines, *VIGS-NbKNAT7* lines did not show significant variation in the glycosyl composition of non-cellulosic fraction. Only a minor decrease in glucose monomer yield was observed in *VIGS-NbKNAT7* lines as compared to control lines. At the same time, a slight increase in the proportion of galacturonic acid (GalA) was observed which indicates increased xylan substitutions.

Immunodetection of hemicellulose and lignin deposition in transgenic tobacco stems

To understand the deposition of xylan and xyloglucan in the stems of VIGS plants, we used specific antibodies targeted to different cell wall components as described earlier (Zhu et al. 2010). To detect xylan deposition, we used LM10 monoclonal antibody that is known to bind less branched (1-4)-β-D-xylans (McCartney et al. 2005). We observed LM10-labeled xylan only in secondary cell

Table 1 Glycosyl composition analysis of stems of control and VIGS lines for genes *NbDUF579* and *NbKNAT7*

Sample	Glycosyl residue (mol%)[A]									
	Arabinose (Ara)	Ribose (Rib)	Rhamnose (Rha)	Fucose (Fuc)	Xylose (Xyl)	OMe-Glucuronic Acid (OMe-GlcA)	Galacturonic acid (GalA)	Mannose (Man)	Galactose (Gal)	Glucose (Glc)
VIGS control	–	–	1.4^{c}	–	88.0^{a}	1.2^{a}	1.7^{c}	2.0^{a}	0.7^{b}	5.1^{b}
VIGS-*NbDUF579*	0.8	–	2.1^{a}	–	59.9^{b}	0.8^{b}	5.4^{a}	1.9^{a}	2.3^{a}	27.0^{a}
VIGS-*NbKNAT7*	0.7	–	1.9^{b}	–	87.8^{a}	0.6^{b}	3.1^{b}	1.3^{b}	1.0^{b}	3.9^{b}

Means within column followed by the same letters are not significantly different ($p = 0.01$, ANOVA, post hoc Scheffe's test)

– Not detected

[A] Values are expressed as mole percent of total carbohydrate

wall in developing xylem of control plants. Relatively strong fluorescence signal was observed in VIGS control plants, whereas weak signal was observed in *VIGS-NbDUF579* plants (Fig. 6a), indicating a reduction of xylan deposition in cell walls of *VIGS-NbDUF579* plants; whereas *VIGS-NbKNAT7* stems showed slight decrease in LM10 fluorescence as compared to control stems. Similar decrease in FITC fluorescence signal was observed in *RNAi* lines of tobacco downregulated for genes *NbDUF579* and *NbKNAT7* (Fig. 6b). In overexpression lines, moderate increase in FITC fluorescence signal was observed in tobacco lines overexpressing gene *NbDUF579*, indicating increased xylan deposition in cell walls, while no significant increase in LM10 fluorescence was observed in tobacco lines overexpressing gene *NbKNAT7* (Fig. 6c).

To monitor xyloglucan deposition, stem sections were labeled with LM15, which binds strongly to non-fucosylated xyloglucan (Marcus et al. 2008). A strong FITC signal was observed in cortex region of VIGS control plants (Fig. 7a). A slight decrease in fluorescence signal was observed in *VIGS-NbDUF579* and *VIGS-NbKNAT7* plants, indicating a reduced xyloglucan deposition in these lines. Similar decrease in FITC fluorescence signal was observed in *RNAi* lines of tobacco for gene *NbDUF579* and *NbKNAT7* (Fig. 7b). Similar to our study, Jensen et al. (2011) observed reduced deposition of xyloglucan in *Arabidopsis* double mutant for DUF579, *irx15 irx15-L*. While increased FITC fluorescence signal was observed in tobacco lines overexpressing *NbDUF579* and *NbKNAT7* genes indicating increased xyloglucan deposition in fiber walls (Fig. 7c).

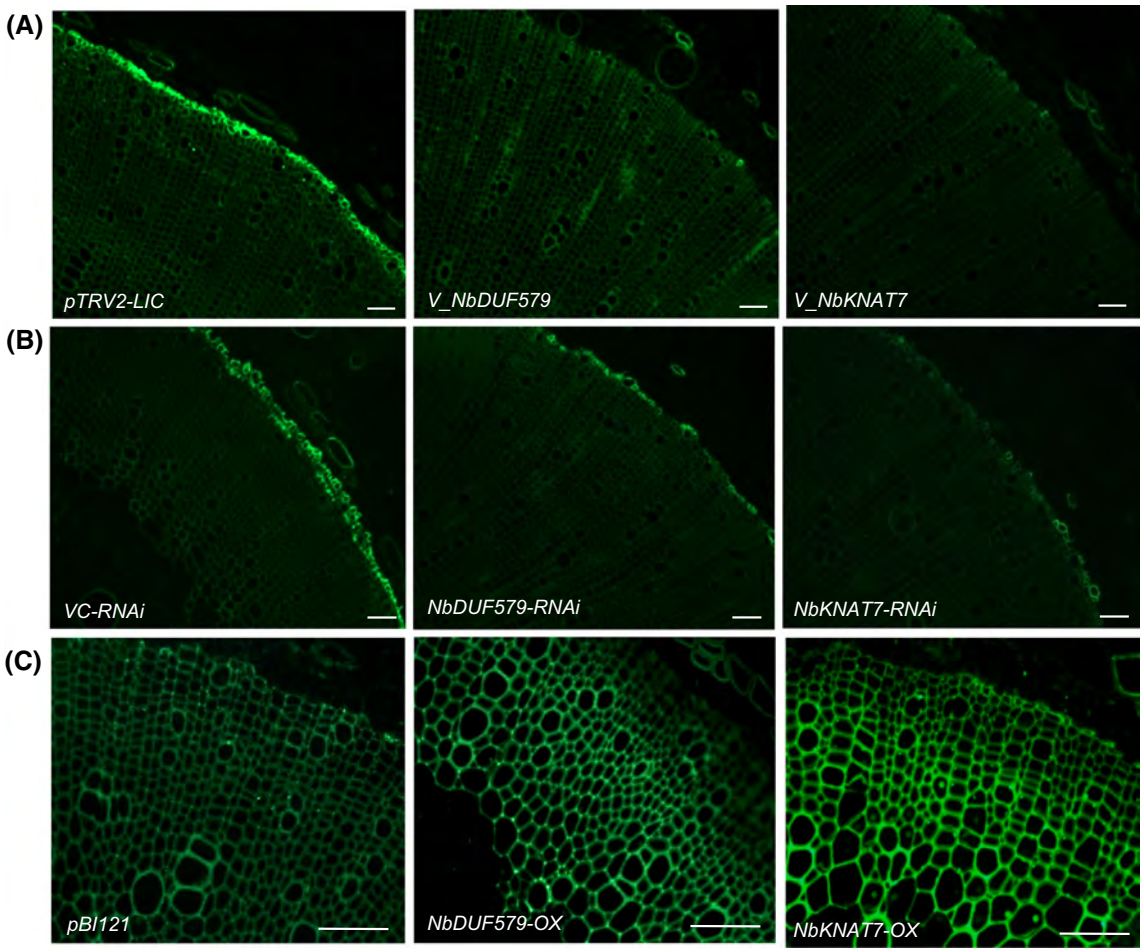

Fig. 6 FITC fluorescence from LM10-labeled stem sections of control and transgenic lines of tobacco. FITC signal indicates xylan deposition in cell walls. **a** FITC fluorescence from LM10-labeled stem sections of control (pTRV2-LIC), *V_NbDUF579* (*VIGS_NbDUF579*) and *V_NbKNAT7 (VIGS_NbKNAT7)* plants; **b** FITC fluorescence from LM10-labeled stem sections of vector control (VC), *NbDUF579-RNAi* and *NbKNAT7-RNAi* lines of tobacco; **c** FITC fluorescence from LM10-labeled stem sections of control (pBI121), *NbDUF579*-OX and *NbKNAT7*-OX lines of tobacco. Sections were taken from third internode from base (5.2 mm dia.). *Bar* 100 µm

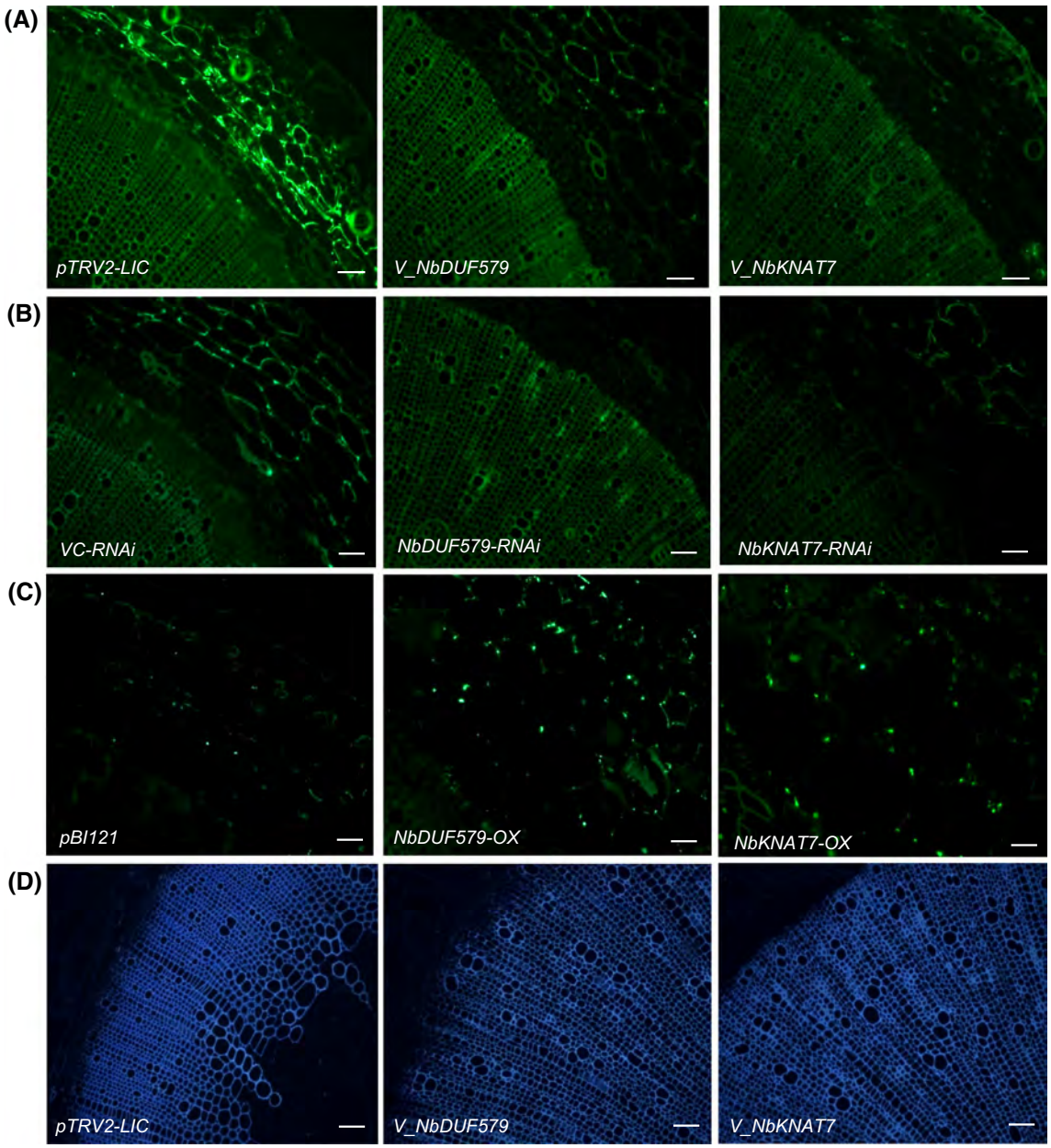

Fig. 7 FITC fluorescence from LM15-labeled stem sections of control and transgenic lines of tobacco. FITC signal indicates xyloglucan deposition in cell wall. **a** FITC fluorescence from LM15-labeled stem sections of control (pTRV2-LIC), *V_NbDUF579* (*VIGS_NbDUF579*) and *V_NbKNAT7 (VIGS_NbKNAT7)* plants; **b** FITC fluorescence from LM15-labeled stem sections of vector control (VC), *NbDUF579-RNAi* and *NbKNAT7-RNAi* lines of tobacco; **c** FITC fluorescence from LM15-labeled stem sections of control (pBI121), *NbDUF579*-OX and *NbKNAT7*-OX lines of tobacco; **d** Lignin deposition in stems of control (pTRV2-LIC), *V_NbDUF579* (*VIGS_NbDUF579*) and *V_NbKNAT7 (VIGS_NbKNAT7)* plants. The level of lignin deposition in secondary xylem cells is indicated by the intensity of *blue* autofluorescence signals from UV-illuminated sections. *Bar* 100 μm

To monitor lignin deposition, we observed UV-induced autofluorescence. A strong and uniform autofluorescence signal was observed in the secondary xylem tissues of UV-illuminated sections of control lines, while the signal was uneven in *VIGS-NbDUF579* and *-NbKNAT7* plants indicating disturbed lignin deposition in secondary cell wall leading to thin walls (Fig. 7d).

Cell wall composition and glucose yield

There was no significant difference in the amount of lignin in the cell walls of *VIGS-NbDUF579* and *-NbKNAT7* lines with respect to vector control lines (Table 2). The amount of cellulose did not change in *VIGS-NbKNAT7* lines as compared to control (Table 2), while *VIGS-NbDUF579* lines showed increased proportions of cellulose (27 %

Table 2 Lignin and cellulose contents in stems of control and VIGS lines of tobacco

Sample	Ave. corrected lignin (%)	Ave. cellulose content (%)
Control	22.5	30.7[c]
VIGS-*NbDUF579*	21.6	39.1[a]
VIGS-*NbKNAT7*	20.7	32.8[b]

Means within column followed by the same letters are not significantly different ($p = 0.01$, ANOVA, post hoc Scheffe's test)

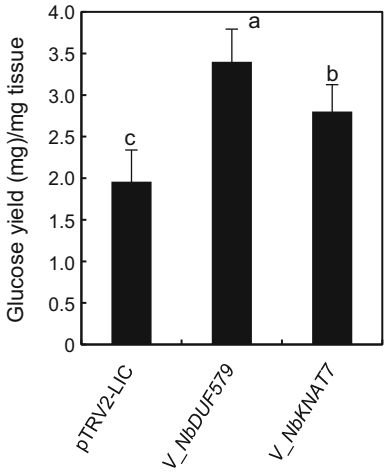

Fig. 8 Glucose release from acetonitrile-washed cell wall residues of control (*pTRV2-LIC*), *V_NbDUF579* (*VIGS_NbDUF579*) and *V_NbKNAT7 (VIGS_NbKNAT7)* tobacco plants. *Bars* are mean ± SE of 12 observations. *Bars* denoted by the *same letter* are not significantly different ($p = 0.01$, ANOVA, post hoc Scheffe's test)

increase) as compared to that of control plants. Contrary to our findings, a slight reduction in cellulose content was observed in double mutants of *Arabidopsis* (*irx15 irx15-L*) (Brown et al. 2011).

Cell wall sugar release from stems of control and VIGS lines was calculated using phenol–sulfuric acid method as reported earlier (DuBois et al. 1956). The amount of glucose release was significantly higher from stems of both types of VIGS lines as compared to control lines (Fig. 8). Significantly higher glucose release was observed in *VIGS-NbDUF579* lines (74.5 % increase over control). Similarly, *VIGS-NbKNAT7* lines showed a 40 % increase in glucose release from cell wall residue as compared to control. The increase in cell wall sugar release in both types of VIGS lines could be attributed to decreased secondary cell wall thickening and an overall decrease in xylan content. Increase in sugar release is a highly desired property of cell walls for efficient bioethanol production. Similar to our findings, Brown et al. (2011) earlier reported a 46 % increase in sugar release in *Arabidopsis* single (*irx15*) and double mutants (*irx15 irx15-L*) with reduced xylan and xyloglucan deposition. Economically feasible production of bioethanol from lignocellulosic feedstocks depends on their efficiency for saccharification, requiring minimum energy, intensive mechanical and/or chemical agents during pretreatments (Nookaraju et al. 2013). Similar to present study, downregulation of xylan synthesis and substitutions also showed a potential for increased sugar production or saccharification.

Conclusion

The two selected genes *NbDUF579* and *NbKNAT7* when downregulated through transient VIGS system resulted in increased xylem proliferation with thin-walled cells. To confirm the results obtained from VIGS system, we generated stable *RNAi* and overexpression lines of tobacco for both *NbDUF579* and *NbKNAT7* genes. Consistent with the VIGS results, the silencing of *NbDUF579* and *NbKNAT7* genes through RNA interference did not result in any adverse phenotypic variations in terms of plant height, internodes number and stem girth when compared to control plants. However, analyses of xylem area and cell wall thickness showed same phenotypic pattern as we observed in VIGS lines. At the same time, we observed opposite phenotypes for both *NbDUF579* and *NbKNAT7* overexpression lines, where all the tested lines showed significant increase in xylem wall thickness compared to vector control plants (Fig. 3). This observation is in support of the function of *DUF579* gene in secondary wall biosynthesis (Jensen et al. 2011; Brown et al. 2011). Contrary to earlier reports on KNAT7 function in Arabidopsis (Li et al., 2012), we report it as a positive regulator of secondary cell wall formation in tobacco as indicated by thinner cell walls in *KNAT7*-silenced lines. Also, expression profiling of key genes involved in secondary wall cellulose (*CesA4*, *7*, *8*), hemicellulose (*IRX8*, *IRX9*, *IRX14*) and lignin (*4CL*, *CCR*, *COMT*) synthesis showed reduced and enhanced expression of these genes in *RNAi* lines and overexpression lines, respectively, over vector control plants.

Author contribution statement SKP and AN conducted most of the experiments, analyzed data, and wrote the article; TF did specific experiments and analyzed the microscopy data; SP did glycome profiling. CPJ planned the experiments, interpreted results, wrote and edited the article, provided guidance, and financial support for this research.

Acknowledgments This work was partially supported by the World Class University project of the Ministry of Science and Technology of South Korea (R31-2009-000-20025-0) and the National Science Foundation, USA to "Wood- to-Wheels" (W2 W) program's "Sustainable Forest-Based Biofuel Pathways to Hydrocarbon Transportation Fuels" project at Michigan Technological University (grant number # 1230803). We wish to thank Dr. Xiaohong Zhu who performed initial VIGS screening. Glycome profiling studies were supported by BioEnergy Science Center (BESC) administered by Oak Ridge National Laboratory and funded by a grant (DE-AC05-00OR22725) from the Office of Biological and Environmental Research, Office of Science, United States, Department of Energy. The development of various CCRC series of cell wall glycan-directed monoclonal antibodies was supported by the NSF Plant Genome Program (DBI-0421683 and IOS-0923992). The authors declare no conflict of interests.

References

Bombarely A, Rosli HG, Vrebalov J, Moffett P, Mueller LA, Martin GB (2012) A draft genome sequence of *Nicotiana benthamiana* to enhance molecular plant-microbe biology research. Mol Plant Microbe Interact 25:1523–1530

Braam J (1999) If walls could talk. Curr Opin Plant Biol 2:521–524

Brown DM, Wightman R, Zhang Z, Atanassov I, Bukowski JP, Tryfona T, Dupree P, Turner SR (2011) Arabidopsis genes IRREGULAR XYLEM (IRX15) and IRX15L encode DUF579 containing proteins that are essential for normal xylan deposition in the secondary cell wall. Plant J 66:387–400

Burch-Smith TM, Anderson JC, Martin GB, Dinesh-Kumar SP (2004) Applications and advantages of virus-induced gene silencing for gene function studies in plants. Plant J 39:734–746

DeMartini JD, Pattathil S, Avci U, Szekalski K, Mazumder K et al (2011) Application of monoclonal antibodies to investigate plant cell wall deconstruction for biofuels production. Energ Environ Sci 4(10):4332–4339

Dong Y, Burch-Smith TM, Liu Y, Mamillapalli P, Dinesh-Kumar SP (2007) A ligation-independent cloning tobacco rattle virus vector for high-throughput virus-induced gene silencing identifies roles for NbMADS4-1 and -2 in floral development. Plant Physiol 145:1161–1170

DuBois M, Gilles K, Hamilton J, Rebers P, Smith F (1956) Colorimetric method for determination of sugars and related substances. Anal Chem 28(3):350–356

Evans RJ, Milne TA (1987) Molecular characterization of the pyrolysis of biomass. 1. Fundamentals. Energy Fuels 1(2):123–137

Jensen JK, Kim H, Cocuron JC, Orler R, Ralph J, Wilkerson CG (2011) The DUF579 domain containing proteins IRX15 and IRX15-L affect xylan synthesis in *Arabidopsis*. Plant J 66:387–400

Jones DA, Takemoto D (2004) Plant innate immunity: direct and indirect recognition of general and specific pathogen-associated molecules. Curr Opin Immunol 16:48–62

Joshi CP, Thammannagowda S, Fujino T, Gou JQ, Avci U, Haigler CH, McDonnell LM, Mansfield SD, Mengesha B, Carpita NC, Harris D, Debolt S, Peter GF (2011) Perturbation of wood cellulose synthesis causes pleiotropic effects in transgenic aspen. Mol Plant 4(2):331–345

Li E, Bhargava A, Qiang WY, Friedmann MC, Forneris N, Savidge RA, Johnson LA, Mansfield SD, Ellis BE, Douglas CJ (2012) The class II KNOX gene KNAT7 negatively regulates secondary wall formation in *Arabidopsis* and is functionally conserved in *Populus*. New Phytol 194:102–115

Liu Y, You S, Taylor-Teeples M, Li WHL, Schuetz M, Brady SM, Douglas CJ (2014) BEL1-LIKE HOMEODOMAIN6 and KNOTTED ARABIDOPSIS THALIANA7 interact and regulate secondary cell wall formation via repression of REVOLUTA. Plant Cell 26:4843–4861

Lu R, Martin-Hernandez AM, Peart JR, Malcuit I, Baulcombe DC (2003) Virus-induced gene silencing in plants. Methods 30:296–303

Marcus S, Verhertbruggen Y, Herve C, Ordaz-Ortiz J, Farkas V, Pedersen H, Willats W, Knox JP (2008) Pectic homogalacturonan masks abundant sets of xyloglucan epitopes in plant cell walls. BMC Plant Biol 8:60

McCartney L, Marcus SE, Knox JP (2005) Monoclonal antibodies to plant cell wall xylans and arabinoxylans. J Histochem Cytochem 53:543–546

Merkle R, Poppe I (1994) Carbohydrate composition analysis of glycoconjugates by gas-liquid chromatography/mass spectrometry. Methods Enzymol 230:1–15

Nookaraju A, Pandey SK, Bae HJ, Joshi CP (2013) Designing cell walls for improved bioenergy production. Mol Plant 6:8–13

Pattathil S, Avci U, Hahn MG (2012) Immunological approaches to plant cell wall and biomass characterization: glycome profiling. Methods Mol Biol 908:61–72

Pattathil S, Hahn MG, Dale BE, Chundawat SPS (2015) Insights into plant cell wall structure, architecture, and integrity using glycome profiling of native and AFEXTM-pre-treated biomass. J Exp Bot 66:4279–4294

Pogrebnyak N, Golovkin M, Andrianov V, Spitsin S, Smirnov Y, Egolf R, Koprowski H (2005) Severe acute respiratory syndrome (SARS) S protein production in plants: development of recombinant vaccine. Proc Natl Acad Sci USA 102:9062–9067

Robertson D (2004) VIGS vectors for gene silencing: many targets, many tools. Annu Rev Plant Biol 55:495–519

Scheffe H (1959) The analysis of variance. Wiley, New York

Scheible WR, Pauly M (2004) Glycosyltransferases and cellwall biosynthesis: novel players and insights. Curr Opin Plant Biol 7:285–295

Song D, Sun J, Li L (2014) Diverse role of PtrDUF579 proteins in *Populus* and PtrDUG579-1 function in vascular cambium proliferation during secondary growth. Plant Mol Biol 85:601–612

Updegraff DM (1969) Semimicro determination of cellulose in biological materials. Anal Biochem 32:420–424

Vorwerk S, Somerville S, Somerville C (2004) The role of plant cell wall polysaccharide composition in disease resistance. Trends Plant Sci 9:203–209

Wang Z, Chen C, Xu Y, Jiang R, Han Y, Xu Z, Chong K (2004) A practical vector for efficient knockdown of gene expression in rice (*Oryza sativa* L.). Plant Mol Biol Rep 22:409–417

Yong W, Link B, O'Malley R, Tewari J, Hunter CT, Lu CA et al (2005) Genomics of plant cell wall biogenesis. Planta 221:747–751

York WS, Darvill AG, McNeil M, Stevenson TT, Albersheim P (1986) Isolation and characterization of plant cell walls and cell wall components. Methods Enzymol 118:3–40

Zhong R, Lee C, Zhou J, McCarthy RL, Ye ZH (2008) A battery of transcription factors involved in the regulation of secondary cell wall biosynthesis in *Arabidopsis*. Plant Cell 20:2763–2782

Zhu X, Dinesh-Kumar SP (2008) Virus-induced gene silencing (VIGS) to study gene function in plants RNA interference. In: Doran T, Helliwell C (eds) Methods for plants and animals. CABI Publishing, Wallingford, pp 6–49

Zhu X, Pattathil S, Mazumder K, Brehm A, Hahn MG, Dinesh-Kumar SP, Joshi CP (2010) Virus-induced gene silencing offers a functional genomics platform for studying plant cell wall formation. Mol Plant 3:818–833